1984

Vibrational Analysis of the Motion Process of Compressor Ring-Valve Plates

D. Wang

P. Lu

VIBRATIONAL ANALYSIS OF THE MOTION PROCESS OF COMPRESSOR RING-VALVE PLATES

Wang Di-seng, Associate Professor and Head, Compressor Technology Section Xi'an Jiao-Tong University, China

Lu Pin, Research Student, Compressor Technology Section, Xi'an Jiao-Tong University, China

ABSTRACT

Differing from the traditional method of treating the motion of ring valve-plates as translational or inclined motions of rigid bodies, this paper originated from the concept on deformations involved in the motion processes. Emphasis of research is centered on flexural warping vibrations during opening and closing. Mechanical modelling and mathematical interpretions of plate motion with variously positioned spring systems are established, enabling theoretical solutions of model shape functions, stresses and strains. Numerical Computer results of dynamic analyses can be used as basis for improvement of compressor design with regard to reliability. A set of diagramatic representation of the computed circumferential distribution of the instanteneous desplacements, dynamic stresses and velocities of some ring valve-plates of an actual air compressor are hereby presented.

INTRODUCTION

The actual motion of the ring valve-plate of a compresson is a complicated one of a MDOF system. Of particular importance are the flexural-warping vibrations during the opening and closing processes which contribute chiefly to stress fatigue failures. Consequently, intensive study of these deformations and stresses, and the manner in which they depend on the compressor's thermal and mechanical parameters should doubtlessly be of significance in the designing of more efficient, low power-comsumption and reliable compressor.

Valuable work in this respect has been done by numerous famous researchers (J. Simonitsh[1], W. Soedel[2], L.Boswerch[3], T. F.T.Maclaren[4], J.F.Hamilton[5], et al).

This paper offers an approach which differs from the traditional method of treating the valve-plate as being rigid and translational or inclined motions in the respect that deformations are taken into account, thus necessitating more detailed investigations into the actual plate motion. The author's attention is focussed upon the flexural-warping behavior of the vale-plate under pulsative gas forces, spring forces and impact reactions etc. with different spring systems. Mathematical models are established. Accordingly with their general solutions, further provided with a computer program to facilitate numerical computation. An actual compressor is chosen for case study and numerical results with graphical illustrations are obtained for circumferential destributions of deformations velocities and dynamic stress varying with time during the opening and closing processes.

MECHANICAL MODEL

During the opening processes, impacts between the valve-plate and the guard are likely to be slanted owing to factors such as the pulsative nature and nonuniformity gas forces, lubrication viscosity and localized impact reaction etc. These impacts occur at high velocities and within extremely small areas of the valve plate the resulting large local reactions cause flexural-warping vibrations accompanying the rebound of the plate. Motion after inclined impact may be one of the two following patterns, One posibility is a furthur impact occurs between the valve-plate and the guard under pulsative gas pressure, not necessarily at the same location but with reduced impact reaction. Thus, the valve-plate will finally come into a coinciding position with the guard after several damped impact. Another possibility is after the initial inclined impact, the point of impact becomes a support and the valve-plate comes into coincidence with the guard with pulsative rotary motions. The latter is more likely with lower impact velocities. However, irrespective of whichever the case may be, the net result is that the valve-plate is subjected to deformations and dynamic stress non steady-state flexural-warping vibrations during the entire opening process.

Motions during the closing process is of similar nature.

The valve-plate is taken as a thin isotropic homogeneous elastic annular plate attached to a transverse pulsative load which consist of gas forces, spring forces (including those as pre-compression) and instanteneous reactions of slanted impacts etc. The outer circumference of the valve-plate is unrestricted and forms a free-boundry. The characteristics of flexural-warping vibrations depend upon whether the plate is attached to a single large spring or a series of small ones.

MATHEMATICAL MODEL

As shown in illus. 1, the guard is taken as origin of displacement. The plate vibration equations in polar co-ordinates with boundary and initial conditions can be written according to the vibration theory of thin elastic plate as follows

$$D\nabla^4 w(r,\theta,t)+kw(r,\theta,t)+\rho h\frac{\partial^2 w(r,\theta,t)}{\partial t^2}=\tilde{p}(r,\theta,t) \tag{1a}$$

Boundary conditions:
$$\begin{cases} Mr|_{r=R_2}=0 & Vr|_{r=R_2}=0 \\ Mr|_{r=R_1}=0 & Vr|_{r=R_1}=0 \end{cases} \tag{1b}$$

Initial conditions:
$$w(r,\theta,t)\big|_{t=0}=w(r,\theta)$$
$$\frac{\partial w(r,\theta,t)}{\partial t}\Big|_{t=0}=v(r,\theta) \tag{1c}$$

Where $D=Eh^3/12$ is the flexural rigidily of the plate; $w(r,\theta,t)$ the displacement; $\tilde{p}(r,\theta,t)$ the algebraic sum of sustained forces due to pre-compression, gas pressure and impact etc. K the spring stiffness per unit area of plate, Mr and V_r respectively the moment and equvalant shear on circular section of radius r.

I. Plate attached to single large spring

For this case, the spring force may be assumed to be countinuously and uniformity distributed over the whole plate.

1. Eigen frequencies and model shape functions. To obtain the characteristic equations that gives the desired frequencies, $\tilde{P}(r,\theta,t)$ is taken as zero in (1a) and displacements of free vibrations assumed as

$$w(r,\theta,t)=F_{mn}(r)\cdot\begin{Bmatrix}\cos n\theta \\ \sin n\theta\end{Bmatrix}(A_{mn}\cos\omega_{mn}t + B_{mn}\sin\omega_{mn}t) \tag{2}$$

where ω_{mn} is the angular frequency of model shapes with m pitch circle and n pitch diameter, $F_{mn}(r)\cos n\theta$, as well as, $F_{mn}(r)$

$\sin n\theta$ are independent equations of model shape corresponding to the related frequency. Substituting (2) into (1a) and solving, we obtain

$$F_{mn}(r)=\delta_{omn}J_n(\beta_{mn}r/R_2)+\delta_{1mn}Y_n(\beta_{mn}r/R_2)+\delta_{2mn}I_n(\beta_{mn}r/R_2)+\delta_{3mn}K_n(\beta_{mn}r/R_2) \tag{3}$$

where $$(\beta_{mn}/R_2)^4=\frac{\rho h\omega_{mn}-K}{D} \tag{4}$$

and J_n, Y_n, I_n, K_n are respectively N^{th} order Bessel functions of the 1^{st} and 2^{nd} kind with real and imaginary arguments, $\delta_{omn}, \delta_{1mn}, \delta_{2mn}$ and δ_{3mn} are undermined coefficients. A set of homogeneous equations with the four δ_S' as veriables are obtained after substituting (3) into (1b), and, for non-trivial solutions, it is necessary that the determinant of the coefficients be equal to zero, which condition yields the charactristic equations of the desired frequency coefficients

$$\beta_{mn}\begin{pmatrix}m=o,\ 1,2,3,.....\\ n=o,\ 1,2,3,.....\end{pmatrix}$$

$$f(\beta_{mn})=\det(a_{ij})=0,\quad i,j=1,2,3,4 \tag{5}$$

The β_{mn}'s are given by (5) and from (4) we obtain eigen frequencies of the vibratory system

$$f_{mn}=\frac{\omega_{mn}}{2\pi}=\sqrt{\frac{D(\beta_{mn}/R_2)^4+K}{\rho h}} \tag{6}$$

with the corresponding two independent model shape function

$$W_{mn}(r,\theta)=F_{mn}(r)\begin{Bmatrix}\cos n\theta\\ \sin n\theta\end{Bmatrix}=[J_n(\beta_{mn}r/R_2)+\delta_{1mn}Y_n(\beta_{mn}r/R_2)+\delta_{2mn}I_n(\beta_{mn}r/R_2)+\delta_{3mn}K_n(\beta_{mn}r/R_2)]\cdot\begin{Bmatrix}\cos n\theta\\ \sin n\theta\end{Bmatrix} \tag{7}$$

where

$$\delta_{1mn}=-\begin{vmatrix}a_{11}&a_{13}&a_{14}\\ a_{21}&a_{23}&a_{24}\\ a_{31}&a_{33}&a_{34}\end{vmatrix}\Big/\Delta_{mn},\quad \delta_{2mn}=-\begin{vmatrix}a_{12}&a_{11}&a_{14}\\ a_{22}&a_{21}&a_{24}\\ a_{32}&a_{31}&a_{34}\end{vmatrix}\Big/\Delta_{mn}$$

$$\delta_{3mn}=-\begin{vmatrix}a_{12}&a_{13}&a_{11}\\ a_{22}&a_{23}&a_{21}\\ a_{32}&a_{33}&a_{31}\end{vmatrix}\Big/\Delta_{mn},\quad \Delta_{mn}=\begin{vmatrix}a_{12}&a_{13}&a_{14}\\ a_{22}&a_{23}&a_{24}\\ a_{32}&a_{33}&a_{34}\end{vmatrix} \tag{8}$$

2. Analysis of Vibration and Dynamic Stress

The excitation forces in (1a) and (1c) may be terms of these model functions, in view of the orthogonality of the model shape function

$$\int_{R_1}^{R_2} rF_{mn}(r)F_{\ell n}(r)dr=\begin{cases}\int_{R_1}^{R_2} rF_{mn}^2(r), & m=\ell\\ 0, & m\neq\ell\end{cases} \tag{9}$$

$$\text{Let}\begin{bmatrix}F_s(g)\\ F_c(g)\end{bmatrix}_{mn}=\int_{R_1}^{R_2}\int_0^{2\pi} rF_{mn}(r)\ g\cdot\begin{bmatrix}\sin n\theta\\ \cos n\theta\end{bmatrix}drd\theta \tag{10}$$

$$\tilde{p}(r,\theta,t)=\sum_{m=0}^{\infty}\sum_{n=0}^{\infty}[C_{smn}(t)\sin n\theta+C_{cmn}(t)\cos n\theta]\cdot\frac{F_{mn}(r)}{G_{mn}} \tag{11}$$

where $$\begin{bmatrix}C_{smn}(t)\\ C_{cmn}(t)\end{bmatrix}=\begin{bmatrix}F_s[p(r,\theta,t)]\\ F_c[p(r,\theta,t)]\end{bmatrix}_{mn} \tag{12}$$

$$w_o(r,\theta)=\sum_{m=0}^{\infty}\sum_{n=0}^{\infty}[U_{smn}\sin n\theta+U_{cmn}\cos n\theta]\frac{F_{mn}(r)}{G_{mn}} \tag{13}$$

where $$\begin{bmatrix}U_{smn}\\ U_{cmn}\end{bmatrix}=\begin{bmatrix}F_s[w_o(r,\theta)]\\ F_c[w_o(r,\theta)]\end{bmatrix}_{mn} \tag{14}$$

$$v_o(r,\theta)=\sum_{m=0}^{\infty}\sum_{n=0}^{\infty}[V_{smn}\sin n\theta+V_{cmn}\cos n\theta]\frac{F_{mn}(r)}{G_{mn}} \tag{15}$$

where $$\begin{bmatrix}V_{smn}\\ V_{emn}\end{bmatrix}=\begin{bmatrix}F_s[v_o(r,\theta)]\\ F_c[v_o(r,\theta)]\end{bmatrix}_{mn} \tag{16}$$

and in (11) (13) (15)

$$G_{mn}=\begin{cases}\pi\int_{R_1}^{R_2} rF_{mn}^2(r)dr, & n\neq o\\ 2\pi\int_{R_1}^{R_2} rF_{mo}^2(r)\,dr, & n=o\end{cases} \tag{17}$$

Take the displacement and velocity respectively as

$$w(r,\theta,t)=\sum_{m=0}^{\infty}\sum_{n=0}^{\infty}[T_{smn}(t)\sin n\theta+T_{cmn}(t)\cos n\theta]\cdot F_{mn}(r) \tag{18}$$

$$v(r,\theta,t)=\frac{\partial w(r,\theta,t)}{\partial t}=\sum_{m=0}^{\infty}\sum_{n=0}^{\infty}[T'_{smn}(t)\sin n\theta+T'_{cmn}(t)\cos n\theta]F_{mn}(r) \tag{19}$$

By substituting (11) and (18) into (1a) and solving, with (14) and (16), we obtain

$$\begin{bmatrix}T_{smn}(t)\\T_{cmn}(t)\end{bmatrix}=\frac{1}{G_{mn}}\left\{\begin{bmatrix}U_{smn}\\U_{cmn}\end{bmatrix}-\frac{1}{\rho h\,\omega_{mn}}\int_0^t\begin{bmatrix}C_{smn}(\tau)\\C_{cmn}(\tau)\end{bmatrix}\sin\omega_{mn}\tau d\tau\right\}\cdot\cos\omega_{mn}t+\frac{1}{G_{mn}}\left\{\frac{1}{\omega_{mn}}\begin{bmatrix}V_{smn}\\V_{cmn}\end{bmatrix}+\frac{1}{\rho h\,\omega_{mn}}\int_0^t\begin{bmatrix}C_{smn}(\tau)\\C_{cmn}(\tau)\end{bmatrix}\cos\omega_{mn}\tau d\tau\right\}\sin\omega_{mn}t \tag{20}$$

if in the Stress-strain equations for the bending of the plates, (18) is being substituted, and utilizing the properties of Bessel functions, the following is obtained after some simplification

$$\begin{cases}\sigma_r(r,\theta,t)=-\frac{12D}{h^3}z\left\{\sum_{m=0}^{\infty}\sum_{n=0}^{\infty}[T_{smn}(t)\sin n\theta+T_{cmn}(t)\cos n\theta]\ \overline{HR}_{mn}(r)\right\}\\ \sigma_\theta(r,\theta,t)=\frac{12D}{h^3}z\left\{\sum_{m=0}^{\infty}\sum_{n=0}^{\infty}[T_{smn}(t)\sin n\theta+T_{cmn}(t)\cos n\theta]\ \overline{HQ}_{mn}(r)\right\}\\ \tau_{r\theta}(r,\theta,t)=-D(1-\nu)\frac{12}{h^3}z\left\{\sum_{m=0}^{\infty}\sum_{n=0}^{\infty}[-T_{smn}(t)\cos n\theta+T_{cmn}(t)\sin n\theta]\ \overline{HRQ}_{mn}(r)\right\}\\ \varepsilon_r(r,\theta,t)=-z\sum_{m=0}^{\infty}\sum_{n=0}^{\infty}[T_{smn}(t)\sin n\theta+T_{cmn}(t)\cos n\theta]\cdot\overline{ER}_{mn}(r)\\ \varepsilon_\theta(r,\theta,t)=-z\sum_{m=0}^{\infty}\sum_{n=0}^{\infty}[T_{smn}(t)\sin n\theta+T_{cmn}(t)\cos n\theta]\cdot\overline{EQ}_{mn}(r)\\ \gamma_{r\theta}(r,\theta,t)=-2z\sum_{m=0}^{\infty}\sum_{n=0}^{\infty}[-T_{smn}(t)\cos n\theta+T_{cmn}(t)\sin n\theta]\cdot\overline{ERQ}_{mn}(r)\end{cases} \tag{21}$$

where $-\frac{h}{2}<z\leq\frac{h}{2}$

$$\begin{cases}\overline{HR}_{mn}(r)=\left[\partial_{mn}^2-\frac{n}{r^2}(1-\nu)(1-n)\right]F_{mn}(r)+(1-\nu)\frac{\partial_{mn}}{r}\cdot[\tilde{F}_{mn}(r)-2\delta_{2mn}I_{n+1}(\partial_{mn}r)]-2\partial_{mn}^2[J_n(\partial_{mn}r)+\delta_{1mn}Y_n(\partial_{mn}r)]\\ \overline{HQ}_{mn}(r)=\left[\nu\partial_{mn}^2+\frac{n}{r^2}(1-\nu)(1-n)\right]F_{mn}(r)-(1-\nu)\frac{\partial_{mn}}{r}[\tilde{F}_{mn}(r)-2\delta_{2mn}I_{n+1}(\partial_{mn}r)]-2\nu\partial_{mn}^2[J_n(\partial_{mn}r)+\delta_{1mn}Y_n(\partial_{mn}r)]\\ \overline{HRQ}_{mn}(r)=\frac{n(1-n)}{r^2}F_{mn}(r)+\frac{n\partial_{mn}}{r}[\tilde{F}_{mn}(r)-2\delta_{2mn}I_{n+1}(\partial_{mn}r)]\\ \overline{ER}_{mn}(r)=\left[\partial_{mn}^2-\frac{n}{r^2}(1-n)\right]F_{mn}(r)+\frac{\partial_{mn}}{r}\cdot[\tilde{F}_{mn}(r)-2\delta_{2mn}I_{n+1}(\partial_{mn}r)]-2\partial_{mn}^2[J_n(\partial_{mn}r)+\delta_{1mn}Y_n(\partial_{mn}r)]\\ \overline{EQ}_{mn}(r)=\frac{n(1-n)}{r^2}F_{mn}(r)-\frac{\partial_{mn}}{r}[\tilde{F}_{mn}(r)-2\delta_{2mn}I_{n+1}(\partial_{mn}r)]\\ \overline{ERQ}_{mn}(r)=\overline{HRQ}_{mn}(r)\end{cases} \tag{22}$$

and in (22)

$$\partial_{mn}=\beta_{mn}/R_2 \tag{23}$$

$$\tilde{F}_{mn}(r)=J_{n+1}(\partial_{mn}r)+\delta_{1mn}Y_{n+1}(\partial_{mn}r)+\delta_{2mn}I_{n+1}(\partial_{mn}r)+\delta_{3mn}K_{n+1}(\partial_{mn}r) \tag{24}$$

II. Plate attached to a series of small springs. For this case, the plate may be

modelled as shown in Figure 2, assume the spring force of each spring is distributed over the trapezoidal area of included angle $2\Delta\theta$, where $\theta_o = \frac{2\pi}{N}$ is the angle between the radial bisectors of two adjacent trapezoidal areas (N being the number of springs). Furthermore, assuming that the area of each trapezoidal area and that of the encircled spring area being equal, i, e.

$$\Delta\theta = \frac{\pi d^2}{4(R_2^2 - R_1^2)} \tag{25}$$

where d is the average radius of one small spring. 1. Eigen-frequencies and modal shape functions For the model as shown in Fig. 2, the Rayleigh-Ritz method may be employed to obtain approximate solutions for the eigen-frequencies and corresponding modal shape functions. The apporach of Ritz is to choose functions such as (7) and satisfying free-boundary conditions as admissible functions, in order to obtain the desired solutions to a sufficient degree of accuracy. Suppose the modal shape functions assume the following form:

$$w(r,\theta) = \sum_{m=0}^{s}\sum_{n=1}^{q}\left[A_{mn}\cos n\theta + B_{mn}\sin n\theta\right] F_{mn}(r) + \sum_{m=0}^{s} A_{mo}F_{mo}(r) \tag{26}$$

where the A_{mn}'s and B_{mn}'s are undermined coefficients, of $(s+1)(q+1)+(s+1)\cdot q=(s+1)\cdot(2q+1)$ terms, s and q to be chosen to attain desired accuracy. The maximum potential and kinetic energies of the valve are, respectively,

$$U_{vmax} = \frac{D}{2}\int_0^{2\pi}\int_{R_1}^{R_2}\left\{(\nabla^2 W)^2 - 2(1-\nu)\left[\frac{\partial^2 W}{\partial r^2}\left(\frac{1}{r}\frac{\partial W}{\partial r}+\frac{1}{r^2}\frac{\partial^2 W}{\partial \theta^2}\right) - \left(\frac{1}{r}\frac{\partial^2 W}{\partial r\partial\theta} - \frac{1}{r^2}\frac{\partial W}{\partial\theta}\right)^2\right]\right\} r\,dr\,d\theta \tag{27}$$

$$T_{vmax} = \frac{\omega^2}{2}\int_0^{2\pi}\int_{R_1}^{R_2}\rho h W^2(r,\theta)\, r\,dr\,d\theta \tag{28}$$

and the sums of those of the small springs are,

$$U_{smnx} = \frac{1}{2}\sum_{l=1}^{N}\int_{R_1}^{R_2}\int_{-\Delta\theta}^{\Delta\theta} k_l W^2(r, l\theta_o+\varphi)\, r\,dr\,d\varphi \tag{29}$$

$$T_{smax} = \frac{\omega^2}{2}\sum_{l=1}^{N}\int_{R_1}^{R_2}\int_{-\Delta\theta}^{\Delta\theta} m_l W^2(r, l\theta_o+\varphi)\, r\,dr\,d\varphi \tag{30}$$

where the k_l and m_l ($l=1, \ldots N$) in (29) and (30) are the spring stiffness and mass of the l^{th} spring divided by the trapezoidal area.

Substituting (26) into (27),(28),(29), (30) and by equating the following partial differentials to zero, i, e.

$$\frac{\partial}{\partial A_{ij}}(U_{vmax} + U_{smax} - T_{vmax} - T_{smax}) = 0 \qquad \begin{pmatrix} i=0,\ 1,\ldots s \\ j=0,\ 1,\ldots q \end{pmatrix} \tag{31}$$

$$\frac{\partial}{\partial B_{ij}}(U_{vmax} + U_{smax} - T_{vmax} - T_{smax}) = 0 \qquad \begin{pmatrix} i=0,\ 1,\ldots s \\ j=1,\ 2,\ldots q \end{pmatrix} \tag{32}$$

By rearrangement of (31), we obtain the following (s+1)(q+1) equations

$$\sum_{m=0}^{s}\sum_{n=0}^{q} C_{1mn}^{(ij)} A_{mn} + \sum_{m=0}^{s}\sum_{n=1}^{q} C_{2mn}^{(ij)} B_{mn} = \omega^2\left[\sum_{m=0}^{s}\sum_{n=0}^{q} D_{1mn}^{(ij)} A_{mn} + \sum_{m=0}^{s}\sum_{n=1}^{q} D_{2mn}^{(ij)} B_{mn}\right] \qquad \begin{pmatrix} i=0,1,\ldots s \\ j=0,1,\ldots q \end{pmatrix} \tag{33}$$

where

$$C_{1mn}^{(ij)}=\begin{cases} J_{mn}^{(mn)}\left[\pi D\left(\frac{\beta_{mn}}{R_2}\right)^4+\sum_{l=1}^{N}k_l\left(\Delta\theta+\frac{1}{2n}\cos 2nl\theta_0\cdot\sin 2n\Delta\theta\right)\right], & ij=mn \\ J_{m0}^{(mo)}\left[2\pi D\left(\frac{\beta_{m0}}{R_2}\right)^4+2\sum_{l=1}^{N}k_l\Delta\theta\right], & n=j=o,\ m=i \\ 0 & n=j,\ m\neq i \\ J_{mn}^{(ij)}\sum_{l=1}^{N}k_l\left[\frac{1}{n+j}\cos(n+j)l\theta_0\sin(n+j)\Delta\theta+\frac{1}{n-j}\cos(n-j)l\theta_0\sin(n-j)\Delta\theta\right], & n\neq j \end{cases}$$

$$C_{2mn}^{(ij)}=\begin{cases} 0 & n=j,\ m\neq i \\ J_{mn}^{(mn)}\sum_{l=1}^{N}k_l\left(\frac{1}{2n}\sin 2nl\theta_0\sin 2n\Delta\theta\right), & ij=mn \\ J_{mn}^{(ij)}\sum_{l=1}^{N}k_l\left[\frac{1}{n+j}\sin(n+j)l\theta_0\sin(n+j)\Delta\theta+\frac{1}{n-j}\sin(n-j)l\theta_0\sin(n-j)\Delta\theta\right], & n\neq j \end{cases}$$

$$D_{1mn}^{(ij)}=\begin{cases} J_{m0}^{(mo)}\left[2\pi\rho h+2\sum_{l=1}^{N}m_l\Delta\theta\right], & n=j=0,\ m=i \\ J_{mn}^{(mn)}\left[\pi\rho h+\sum_{l=1}^{N}m_l\left(\Delta\theta+\frac{1}{2n}\cos 2nl\theta_0\sin 2n\Delta\theta\right)\right] & ij=mn \\ 0 & n=j,\ m\neq i \\ J_{mn}^{(ij)}\sum_{l=1}^{N}m_l\left[\frac{1}{n+j}\cos(n+j)l\theta_0\sin(n+j)\Delta\theta+\frac{1}{n-j}\cos(n-j)l\theta_0\sin(n-j)\Delta\theta\right], & n\neq j \end{cases}$$

$$D_{2mn}^{(ij)}=\begin{cases} 0 & n=j,\ m\neq i \\ J_{mn}^{(mn)}\sum_{l=1}^{N}m_l\left[\frac{1}{2n}\sin 2nl\theta_0\sin 2n\Delta\theta\right], & ij=mn \\ J_{mn}^{(ij)}\sum_{l=1}^{N}m_l\left[\frac{1}{n+j}\sin(n+j)l\theta_0\sin(n+j)\Delta\theta+\frac{1}{n-j}\sin(n-j)l\theta_0\sin(n-j)\Delta\theta\right], & n\neq j \end{cases}$$

in which $$J_{mn}^{(ij)}=\int_{R_1}^{R_2} r\,F_{mn}(r)F_{ij}(r)\,dr \qquad (34)$$

Similarly, (s+1)q equations may be obtained by rearranging (32)

$$\sum_{m=0}^{s}\sum_{n=0}^{q}E_{1mn}^{(ij)}A_{mn}+\sum_{m=0}^{s}\sum_{n=1}^{q}E_{2mn}^{(ij)}B_{mn}=\omega^2\left[\sum\sum F_{mn}^{(ij)}A_{mn}+\sum_{m=0}^{s}\sum_{n=1}^{q}F_{2mn}^{(ij)}B_{mn}\right] \qquad \begin{pmatrix} i=o,1,\ldots s \\ j=1,2,\ldots q \end{pmatrix} \qquad (35)$$

where $$E_{1mn}^{(ij)}=C_{2ij}^{(mn)}$$

$$E_{2mn}^{(ij)}=\begin{cases} J_{mn}^{(mn)}\left[\pi D\left(\frac{\beta_{mn}}{R_2}\right)^4+\sum_{l=1}^{N}k_l\left(\Delta\theta-\frac{1}{2n}\cos 2nl\theta_0\cdot\sin 2n\Delta\theta\right)\right] & ij=mn \\ 0 & n=j,\ m\neq i \\ J_{mn}^{(ij)}\sum_{l=1}^{N}k_l\left[\frac{1}{n-j}\cos(n-j)l\theta_0\sin(n-j)\Delta\theta-\frac{1}{n+j}\cos(n+j)l\theta_0\sin(n+j)\Delta\theta\right], & n\neq j \end{cases}$$

$$F_{1mn}^{(ij)}=D_{2ij}^{(mn)}$$

$$F_{2mn}^{(ij)}=\begin{cases} J_{mn}^{(mn)}\left[\pi\rho h+\sum_{l=1}^{N}m_l\left(\Delta\theta-\frac{1}{2n}\cos nl\theta_0\sin 2n\Delta\theta\right)\right], & ij=mn \\ 0 & n=j,\ m\neq i \\ J_{mn}^{(ij)}\sum_{l=1}^{N}m_l\left[\frac{1}{n-j}\cos(n-j)l\theta_0\sin(n-j)\Delta\theta-\frac{1}{n+j}\cos(n+j)l\theta_0\sin(n+j)\Delta\theta\right], & n\neq j \end{cases}$$

By letting

$$\{X\}=[A_{oo},A_{o1},\ldots A_{oq},A_{1o},A_{11},\ldots A_{1q},A_{so},\ldots A_{sq},B_{o1},\ldots B_{oq},\ldots B_{s1},\ldots B_{sq}]^T=[A_{mn}\,|\,B_{mn}]^T \qquad (36)$$

(33) and (35) may be written in matrix form as

$$[K]\{X\} = \omega^2[M]\{X\} \tag{37}$$

where

$$[K]=\begin{bmatrix} C^{(ij)}_{1mn} & C^{(ij)}_{2mn} \\ E^{(ij)}_{1mn} & E^{(ij)}_{2mn} \end{bmatrix} \quad [M]=\begin{bmatrix} D^{(ij)}_{1mn} & D^{(ij)}_{2mn} \\ F^{(ij)}_{1mn} & F^{(ij)}_{2mn} \end{bmatrix} \tag{38}$$

K is symmetric, while M is positive definite, both of order (s+1)(2q+1). Solving (37) is a generalized eigenproblem, after which may be obtained the (s+1)(2q+1) eigenvector (including repeated roots) and the corresponding eigenvectors. We can write the eigenvector corresponding to λ th eigenvalue ω_λ^2 as from (37) in the form

$$\{X\}_\lambda=[A_{\lambda oo},\cdots A_{\lambda oq},\cdots A_{\lambda so},\cdots,A_{sq};\ B_{\lambda o1},\cdots B_{\lambda oq},\cdots B_{\lambda s1},\cdots B_{\lambda sq}]^T \tag{39}$$

In the case of existence of repeated roots, suppose the j^{th} one is repeated. In order that the two independent eigenvectors be orthogonal to each other $\{X\}_{j2}$'may be used to replace $\{X\}_{j2}$ by

$$\{X\}_{j2'}=\{X\}_{j1}-\frac{\{X\}^T_{j1}[M]\{X\}_{j2}}{\{X\}^T_{j1}[K]\{X\}_{j2}}\{X\}_{j2} \tag{40}$$

Hence, if repeated roots exist, the model shape function corresponding to the eigenvector modified according to (40) becomes

$$W_\lambda(r,\theta)=\sum_{m=0}^{s}\sum_{n=1}^{q}(A_{\lambda mn}\cos n\theta+B_{\lambda mn}\sin n\theta)F_{mn}(r)+\sum_{m=0}^{s}A_{\lambda mo}F_{mo}(r) \tag{41}$$

with the orthogonality property

$$\int_{R_1}^{R_2}\int_0^{2\pi} rW_\lambda(r,\theta)W_\beta(r,\theta)\,dr\,d\theta$$

$$=\begin{cases} 2\pi\sum_{m=0}^{s}(A_{\lambda mo})^2\int_{R_1}^{R_2}rF^2_{mn}(r)dr \\ +\pi\sum_{m=0}^{s}\sum_{n=1}^{q}[A^2_{\lambda mn}+B^2_{\lambda mn}]\int_{R_1}^{R_2}rF^2_{mn}(r)dr=G_\lambda \quad (\lambda=\beta) \\ 0 \qquad \lambda\neq\beta \end{cases} \tag{42}$$

2. Analysis of Vibrations and Dynamic Stresses. The excitation force may be expanded in terms of the modal shape functions as

$$\tilde{p}(r,\theta,t)=\sum_{\lambda=1}^{\Lambda}C_\lambda(t)W_\lambda(r,\theta) \tag{43}$$

where

$$C_\lambda(t)=\frac{\sum_{m=0}^{s}A_{\lambda mo}C_{cmo}(t)+\sum_{m=0}^{s}\sum_{n=1}^{q}[A_{\lambda mn}C_{cmn}(t)+B_{\lambda mn}C_{smn}(t)]}{G_\lambda} \tag{44}$$

and $C_{cmn}(t)$, $C_{smn}(t)$ are those in (12) when $\Lambda \leqslant (s+1)(2q+1)$

$$W_o(r,\theta)=\sum_{\lambda=1}^{\Lambda}U_\lambda W_\lambda(r,\theta) \tag{45}$$

where

$$U_\lambda=\frac{\sum_{m=0}^{s}A_{\lambda mo}U_{smo}+\sum_{m=0}^{s}\sum_{n=1}^{q}[A_{\lambda mn}U_{cmn}+B_{\lambda mn}U_{smn}]}{G_\lambda} \tag{46}$$

in which U_{smn}, and U_{cmn} are those in (14).

$$V_o(r,\theta)=\sum_{\lambda=1}^{\Lambda}V_\lambda W_\lambda(r,\theta) \tag{47}$$

where

$$V_\lambda=\frac{\sum_{m=0}^{s}A_{\lambda mo}V_{\lambda mo}+\sum_{m=0}^{s}\sum_{n=1}^{q}[A_{\lambda mn}V_{cmn}+B_{\lambda mn}V_{smn}]}{G_\lambda} \tag{48}$$

in which V_{smn} and V_{cmn} are those in (16).

Displacements and Velocities,

$$w(r,\theta,t)=\sum_{\lambda=1}^{\Lambda}\left[U_\lambda\cos\omega_\lambda t+\frac{V_\lambda}{\omega_\lambda}\sin\omega_\lambda t+\tau_\lambda(t)\right]\ W_\lambda(r,\theta)$$

$$=\sum_{\lambda=1}^{\Lambda}T_\lambda(t)\ W_\lambda(r,\theta) \qquad (49)$$

$$v(r,\theta,t)=\sum_{\lambda=1}^{\Lambda}\left[-U_\lambda\omega_\lambda\sin\omega_\lambda t+V_\lambda\cos\omega_\lambda t+\tau_\lambda'(t)\right]W_\lambda(r,\theta) \qquad (50)$$

where

$$\begin{bmatrix}\tau_\lambda(t)\\ \tau_\lambda'(t)\end{bmatrix}=\frac{1}{\rho h}\left\{\begin{bmatrix}-\frac{\cos\omega_\lambda t}{\omega_\lambda}\\ \sin\omega_\lambda t\end{bmatrix}\int_0^t C_\lambda(\tau)\sin\omega_\lambda\tau d\tau\right.$$

$$\left.+\begin{bmatrix}\frac{\sin\omega_\lambda t}{\omega_\lambda}\\ \cos\omega_\lambda t\end{bmatrix}\int_0^t C_\lambda(\tau)\cos\omega_\lambda\tau d\tau\right\}$$

Stresses and strains

these are given by

$$\left\{\begin{aligned}
\sigma_r(r,\theta,t)&=-\frac{12DZ}{h^3}\left\{\sum_{\lambda=1}^{\Lambda}T_\lambda(t)\left[\sum_{m=0}^{s}\sum_{n=1}^{q}(A_{\lambda mn}\cos n\theta\right.\right.\\
&\left.\left.+B_{\lambda mn}\sin n\theta)\ \overline{HR}_{mn}+\sum_{m=0}^{s}A_{\lambda mo}\overline{HR}_{mo}\right]\right\}\\
\sigma_\theta(r,\theta,t)&=-\frac{12DZ}{h^3}\left\{\sum_{\lambda=1}^{\Lambda}T_\lambda(t)\left[\sum_{m=0}^{s}\sum_{n=1}^{q}(A_{\lambda mn}\cos n\theta\right.\right.\\
&\left.\left.+B_{\lambda mn}\sin n\theta)\overline{HQ}_{mn}+\sum_{m=0}^{s}A_{\lambda mo}\overline{HQ}_{mo}\right]\right\}\\
\tau_{r\theta}(r,\theta,t)&=-D(1-\nu)\frac{12Z}{h^3}\left\{\sum_{\lambda=1}^{\Lambda}T_\lambda(t)\sum_{m=0}^{s}\sum_{n=1}^{q}(A_{\lambda mn}\sin n\theta\right.\\
&\left.-B_{\lambda mn}\cos n\theta)\ \overline{HRQ}_{mn}\right\} \qquad (51)\\
\varepsilon_r(r,\theta,t)&=-Z\sum_{\lambda=1}^{\Lambda}T_\lambda(t)\left\{\sum_{m=0}^{s}\sum_{n=1}^{q}[A_{\lambda mn}\cos n\theta\right.\\
&\left.+B_{\lambda mn}\sin n\theta]\overline{ER}_{mn}+\sum_{m=0}^{s}A_{\lambda mo}\overline{ER}_{mo}\right\}\\
\varepsilon_\theta(r,\theta,t)&=-Z\sum_{\lambda=1}^{\Lambda}T_\lambda(t)\left\{\sum_{m=0}^{s}\sum_{n=1}^{q}[A_{\lambda mn}\cos n\theta\right.\\
&\left.+B_{\lambda mn}\sin n\theta]\overline{EQ}_{mn}+\sum_{m=0}^{s}A_{\lambda mo}\overline{EQ}_{mo}\right\}\\
\gamma_{r\theta}(r,\theta,t)&=-2Z\sum_{\lambda=1}^{\Lambda}T_\lambda(t)\left\{\sum_{m=0}^{s}\sum_{n=1}^{q}[A_{\lambda mn}\sin n\theta-B_{\lambda mn}\cos n\theta]\right.\\
&\left.\cdot\overline{ERQ}_{mn}\right\}
\end{aligned}\right.$$

where $\overline{HR}_{mn}$, $\overline{HQ}_{mn}$, $\overline{HRQ}_{mn}$, $\overline{EQ}_{mn}$, $\overline{ERQ}_{mn}$, $\overline{ER}_{mn}$ are those in (22) when $-\frac{h}{2}\leqslant Z\leqslant\frac{h}{2}$.

EXCITATION FORCES

with co-ordinate system chosen as shown in Fig.(1a), the excitation forces $\tilde{p}(r,\theta,t)$ may be expressed in the form

$$\tilde{p}(r,\theta,t)=F^*\delta(r-r_0)\delta(\theta-\varphi_0)\delta(t-t_0)+k(H+H_0)$$

$$-\Delta p(r,\theta,t) \qquad (52)$$

where $k(H+H_0)$ is the sum of pre-compression and spring forces on unit area of valve-plate at instant of maximum opening, $F^*\ (r-r_0)\delta(\theta-\varphi_0)\delta(t-t_0)$ the instanteneous impact reaction due to the impact at point $r=r_0$ and $\theta=\varphi_0$ on the plate at instant $t=t_0$, and F^* the average amplitude when the impact is upon the guard and negative upon the valve seat, $\Delta P(r,\theta,t)$ is the gas force. The actual variation of impact force during the extremely short interval ($<\frac{1}{1000}$ sec) of impact is very complicated, but its average valve may be obtained approximately according to impact theory as

$$F^*=\frac{1}{\tau}\int_0^\tau F(t)dt=\frac{1}{\tau}\int_{R_1}^{R_2}\int_0^{2\pi}\rho h[v_1(r,\theta)-v_2(r,\theta)]$$

$$\cdot r dr d\theta \qquad (53)$$

where $\rho h[v_1(r,\theta)-v_2(r,\theta)]$ is the difference of kinetic energies of the plate's differential element before and after the impact, τ being the interval of impact. As shown in Fig. 3, the pressures of the main blow and side blow are obviously of considerable difference owing to loss of pressure during gaseous flow. Supposing that the gas forces vary diminishingly along the plate circumference and systematically with respect to the diameter connecting the points of main blow and side blow, and fur-

ther assuming a constant gas force accross the same θ - section owing to the narrowness of the plate. If p(t) is the main blow force, the circumferential variation of gas force may be expressed as

$$\Delta P(r,\theta,\ t) = p(t)\ E(\theta) \tag{54}$$

Define

$$E(\theta) = \frac{e\ x\ p(-\xi\frac{\theta}{\pi}) + e\ x\ p(-\xi\frac{2\pi-\theta}{\pi})}{1 + e\ x\ P(-2\xi)}$$

$$0 \leqslant \theta \leqslant 2\pi \qquad \xi > 0 \tag{55}$$

as the modifying function, which satisfies

$0 < E(\theta) \leqslant 1$,

$E(\theta) = 1$ at point of main blow ($\theta = o$) and a minimum at point of side blow ($\theta = \pi$). It is also symetrical with respect to the diameter joining points of $\theta = 0$ and $\theta = \pi$. ξ is a damping coefficient depending upon the structure and dimensions of the valve-plate. It can determined experimentally, valued approximately between

$(R_1/R_2)^3$ and $(R_1/R_2)^2$.

p(t) also can be obtained by using the following approximate expression

$$p(t) = \frac{1}{8}\beta\kappa\pi^2\bar{M}^2 p_i\left[\sin(\omega t+\psi_o) + \frac{\lambda}{2}\sin 2(\omega t+\psi_o)\right]^2 \tag{56}$$

where β is the coefficient of lift, κ the heat absolute index, $\bar{M}^2$ the Mach number of valve clearance, p_i the gas pressure in the valve volume, ψ_o the phase angle of crank at opening, t the time from opening of valve, and ω the rotary speed of the compressor.

NUMERICAL COMPUTATION

Based on the theoretical treatment and the equation derived thereof, a program is written for computation of the eigen-frequencies, dynamic displacements and stress of the valve-plate. Comparatively satisfactory results are obtained after assigning numerical values to the parameters of some types of valves.

A simple flow chart is shown below

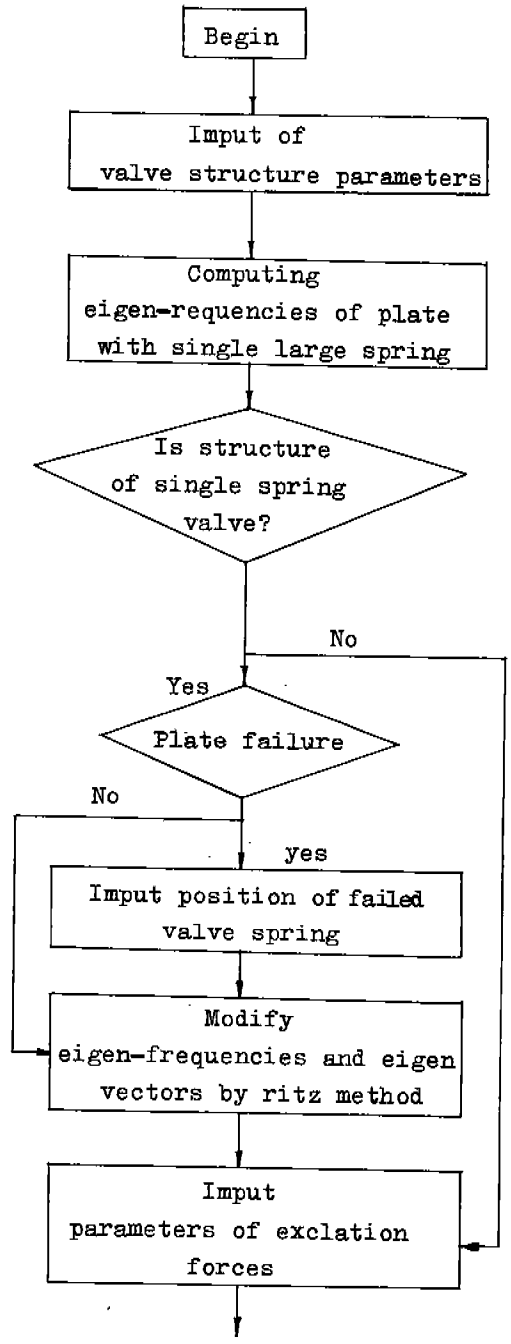

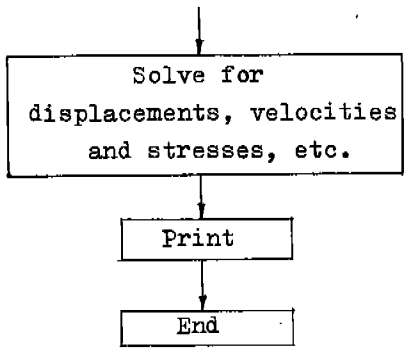

The eigen-frequencies of a valve-plate with a single large spring may be obtained from

$$f_{mn}=\frac{\omega_{mn}}{2\pi}=\frac{1}{2\pi}\sqrt{\frac{D(\beta_{mn}/R_2)^4+k}{\rho h}} \qquad (57)$$

where β_{mn} is a dimensionless coefficient of frequency, and its computed values for valve-plates of various inner/outer deameter ratios are given in table 1.

table 1 - Frequency Coefficient β_{mn} (poisson's ratio $\nu = 0.3$)

m	n	R_1/R_2			
		0.6	0.7	0.8	0.9
0	0	0.0	0.0	0.0	0.0
	1	0.0	0.0	0.0	0.0
	2	1.97999	1.89011	1.80027	1.71283
	3	3.27143	3.13988	2.99737	2.85377
	4	4.48212	4.32396	4.13486	3.93734
	5	5.65003	5.47953	5.24977	4.99898
	6	6.78745	6.61723	6.35366	6.05009
	7	7.90122	7.74096	7.45122	7.09565
	8	8.99642	8.85236	8.54441	8.13804
1	0	3.26417	3.62807	4.29800	5.90196
	1	4.30166	4.68122	5.47316	7.46455
	2	5.71708	6.15152	7.13364	9.68483
	3	6.99595	7.46334	8.60126	11.63646
	4	8.20034	8.65954	9.90914	13.35265
	5	9.38210	9.79018	11.10851	14.89775
	6	10.56738	10.88787	12.23442	16.31639
	7	11.76578	11.97299	13.31047	17.63871
	8	12.97761	13.05788	14.35293	18.88578

For valve-plate of other diameter ratios, β_{mn} can be obtained by interpolation.

Table 1 reveals some of the vibrational characteristies the valve-plate with a single large spring. The valve-plate is a body with a free-boundry. Its motion is the superposition of three components-translational, rigid-body inclination and vibrations. Therefore the system is semipositive and, as a result, there naturally exist zero eigen-values. The modes corresponding to m= o and n= o in table 1 are those of rigid-body translations, while those corresponding to m= o and n= 1 are related to rigid-body inclinations, and, as these motions do not excite vibrations, the frequencies of course equal to zero. It may be seen from (7) that the two afore-mentioned modes, the vibrations of the valve-plate is equivalent to those of mass-spring system with the plate as a mass point. This is to say, treating the plate as rigid actually leaves out all the modes corresponding to deformational vibrations. furthermore, it may be seen from table 1 that the frequency confficients increases rapidly with the pitch cirele number of the modes, with increasing of the eigen-frequencies ($f_{mn} \propto \beta_{mn}^2$).

For a plate of inner diameter 115^{mm} and outer diameter 130^{mm} with six springs of stiffness $228 N/m^2$ equally-spaced circumfer-entially along the plate, it can be simulated by a model with a single large spring or a series of small springs. Its various eigen-frequencies are listed in table 2 .

table 2. Eigen-frequencies of Different spring systems

f_{mn} (HZ) m / n	continuous spring system		Discrete spring system	
	0	1	0	1
0	27	3507	26	3506
1	27	5579	27	5579
2	344	9375	343	9370
3	952	13534	927,977	13199,13896
4	1812	17833	1815	17865
5	2922	22220	2926	22252
6	4282	26639	4192	26129
			4390	27365

We can see that corresponding to each m th mode (m= 0, 1, 2...) there exist two eigen-frequencies. This may be, explained as follows. In the continuous spring system, there are two independent modal shape functions $F_{mn}(r)\cos n\theta$ and $F_{mn}(r)\sin n\theta$, while for the discrete system, the eigen-frequencies change due to change of the systems structure.

Table 3 is for a 110-130mm plate with six small springs of stiffness of 490N/m², the eigen-frequences shown therein are for the cases with all springs intact and with one spring failed.

table 3. Influence of Failure of spring on Eigen-frequencies

f_{mn} (HZ) m / n	all springs intact		one spring fails	
	0	1	0	1
0	39	2049	28	2015
1	40	3204	40	3204 3238
2	268	5397	268 270	5397 5459
3	717 761	7580 8076	724 761	7661 8077
4	1406	10357	1327 1420	10358 10422

table 3 clearly shows that the failure of one spring causes the change of all eigen-frequencies. In addition, pairs of proximate-valued eigne-frequencies appear, the proximity depending on the spring stiffness. These proximate-valued eigen-frequencies will worsen the stability of valve motion and doubtlessly unfavorably influence the compressor's life-span.

Computations are made for the dynamic displacements, stresses etc of the first step in-let motion for a 2V - 6/8 air compresson. The valve consists of three rings the inner valve is equipped with three springs and the middle and outer valve each with six springs. All the springs are of equal stiffness.

The origin of the polar coordinates is placed direct toward the point of main blow. When impact is completed the instant of impact is chosen as origin of time. Figure 5 shows the variations along the average radial circumference of σ_r, σ_θ and $\tau_{r\theta}$, Logarthmic scale is used for the longitudinal ordinate, from which it can be seen that the maximum amplitude of σ_r is about $2 \times 10^7 N/m^2$ while those of σ_θ and $\tau_{r\theta}$ come to the order $2 \times 10^8 N/m^2$ (the yield limit of steel σ_s being $8 \sim 13 \times 10\ N/m^2$). Thus we have reason to believe that σ_θ and $\tau_{r\theta}$ are dominant factors that affect the lifespan of the valve-plate. Owing to its narrowness, bending and twisting will result in large increases of σ_θ and $\tau_{r\theta}$.

The circumferential variations of dynanic stresses σ_θ and displacements w at $\theta = 0$ at various instants after impact with the guard is shown in Figures 6 and 7. Immediately after the impact, violent vibrations occur with inclined motion, with correspondingly high stresses.

As the disturbances are rapidly damped, the amplitudes of vibrations and stresses drops sharply to reach a state of stability, and the plate finally comes to a position of coincidence of the guard.

The high stresses induced by the violent

shocking vibration is the main cause of plate failure. The maximum calculated stress σ_θ is around $3 \times 10^8 N/m^2$ which, although below the yield limit, could lead to stress fatigue when the plate is under such rapidly alternating stresses.
Figure 8 also shows that the point of rebound is higher than other displacements and this causes the plate to vibrate in inclined positions.
Figure 9 shows the displacement of the rebound with varying gas force while other conditions are being kept constant.
It is evident that decrease of gas force results in decrease of velocity after rebound.

DISCUSSIONS

The author's work demonstrates that the dynamic analysis of the valve-plate can be accomplished by the hybrid approach of analytical-numerical methods. Compared with the finite element method, it seems to possess the advantages of high accuracy and reduction of computational work.
Theorectical investigations and results of numerical computations tend to indicate the following:

1. Nonsteady-state flexural-torsional vibrations actually take place during the opening and closing processes of valve-plate motion. The characteristics of these vibrations depend on such factors as the placing of springs, spring constants, relative sizes of valve and valve-plates, the magnitude of compressor's pulsative gas force, revolutionary speed etc.

2. Dynamic stresses σ_θ, σ_r, $\tau_{r\theta}$ are produced by the flexural-torsional vibrations, The magnitude of σ_θ is higher than those of others, thus being the chief cause of radial fatigue fractures.

3. The vibrational characteristies of a multi-small-spring system are closely related to the uniformity of stiffnesses and the number of the small springs. Non-uniformity of spring stiffnesses or the failure of an individual spring will result in the increase of eigen-frequency band width with a loss of stability.

4. The maximum dynamic stresses occur at the instants of successive inclined impacts, judged from the point of view of stress-fatigue, the compressor's revolutionary speed not only direclty influences, the vibrational characteristics, but also indirectly causes change of the loading frequencies of dynamic stresses. It is therefore the designer's chief concern to select the proper revolutionary speed in determining the life-span criterion of the compressor valve plate.

REFERENCES

(1) J. Simonitch, "Mechanical Stresses of Valve Plates on Impact Against Valve Seat and Guard". Procedings of the 1978 Purdue Compressor Technology Conference.

(2) P. Pandeya, W.Soedel, "Analysis of the Influence of Seat-Plating Or Cushioning on Valve Impact Stresses in High Speed Compressors," Proceedings of the 1978 Purdue Compressor Technology Conference.

(3) L.Böswirth, "Hypothesis on the Failure of Spring Loaded Compressor Valve Plates." Proceedings of the 1980 Purdue Compressor Technology Conference.

(4) J.F.T.Maclaren, A.B.Tramschek, I.J.Hussein, B.A.El-Geresy, "Can the Impact Velocities of Suction Valves Be Calculated?" Proceedings of the 1978 Purdue Compressor Technology Conference.

(5) H.K.Reddy, J.F.Hamilton, "Accurate Experimental Determination of Frequencies, Mode Shapes and Dynamic Strains in Plate valves of Reciprocating Compressors," Proceedings of the 1976 Purdue Compressor Technology Conference.

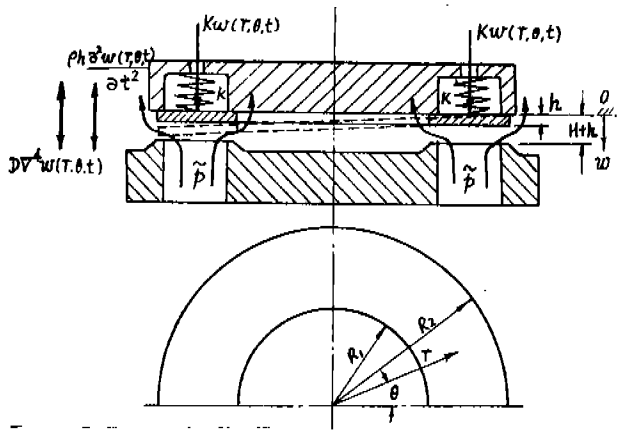

Figure. 1. Load Distribution on Annular valve-plate

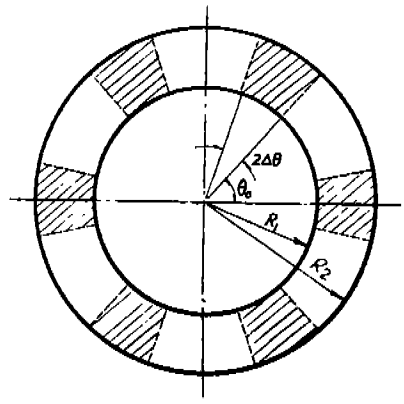

Figure.2. Annular valve-plate attached to series of small springs

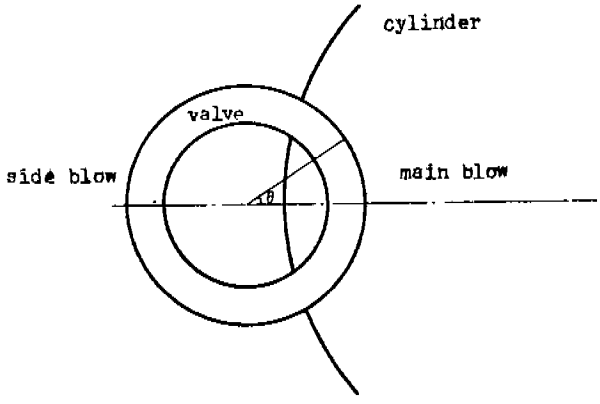

Figure.3. Side-blow through Annular valve-plate

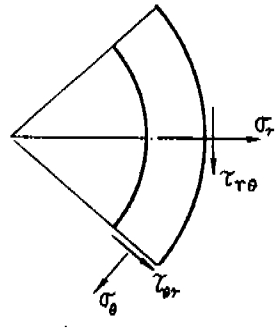

Figure.4. Stress Distribution on valve-plate

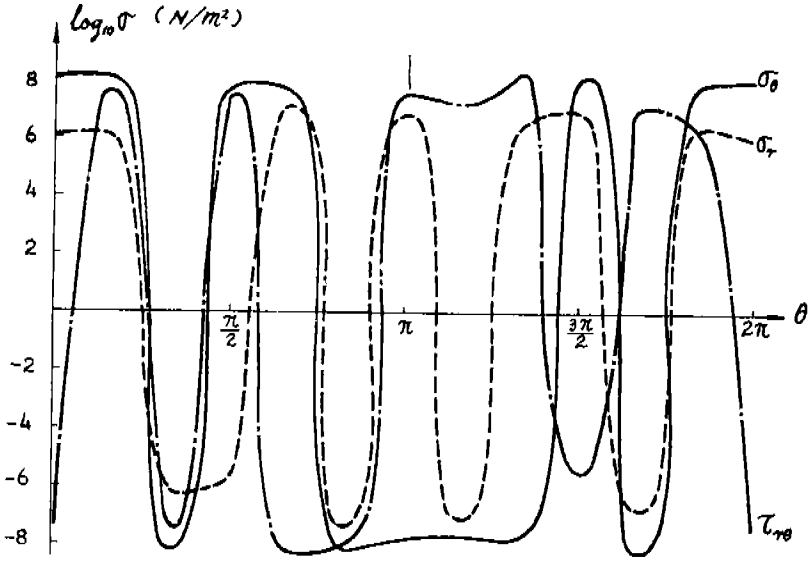

Figure.5. Distribution of σ_θ , σ_r and $\tau_{r\theta}$ on valve-plate at t=0.0005 sec.

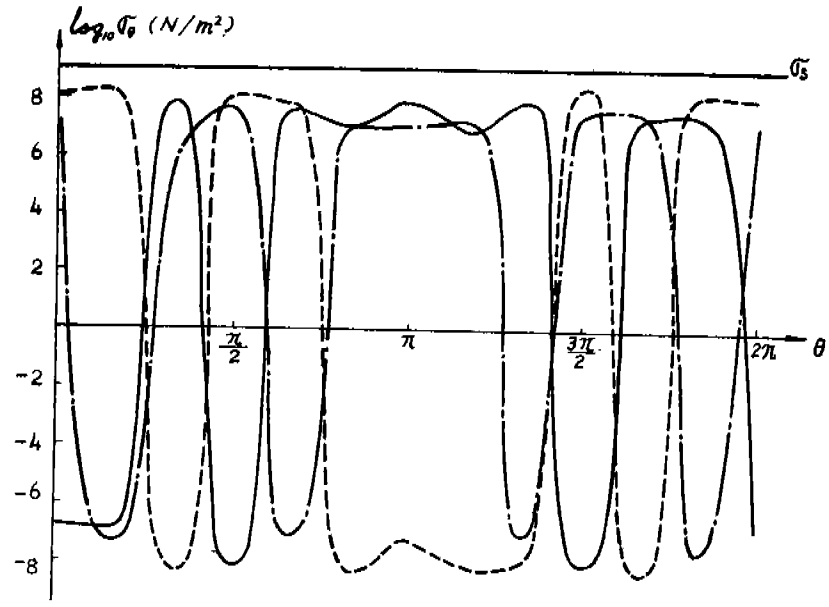

Figure.6. Distributions of Dynamic stresses σ_θ at various instemts of time (impact at θ =0)

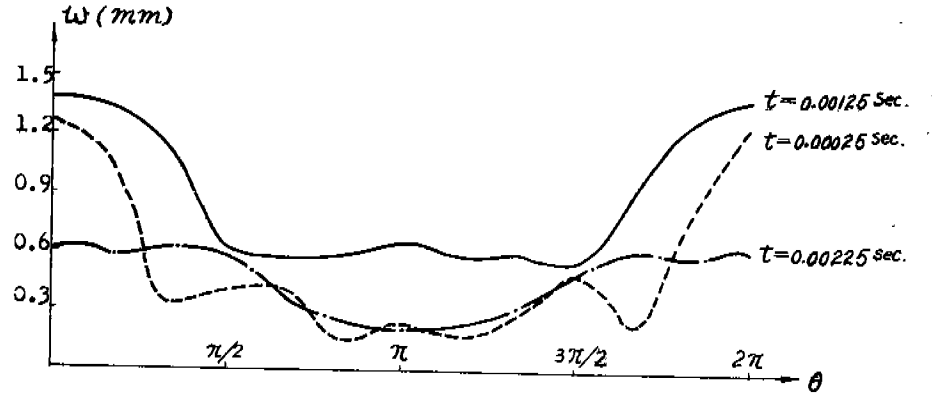

Figure.7. Displacements of valve-plates at various instants of time (impact at θ = 0)

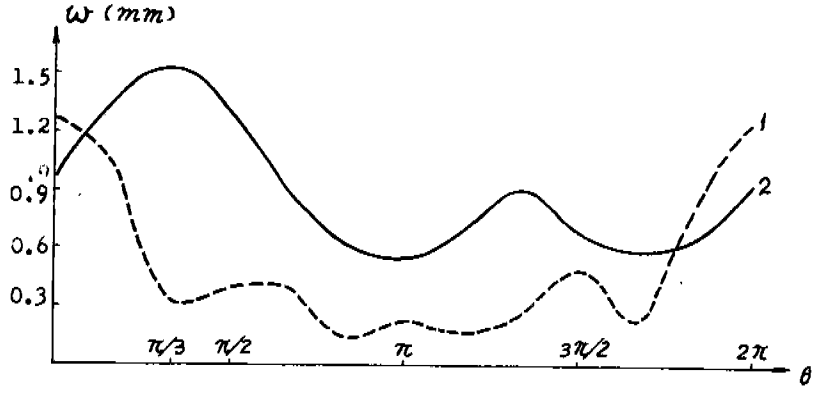

Figure.8. Displacements at various impact positions.
1. θ = 0 2. $\theta = \pi/3$

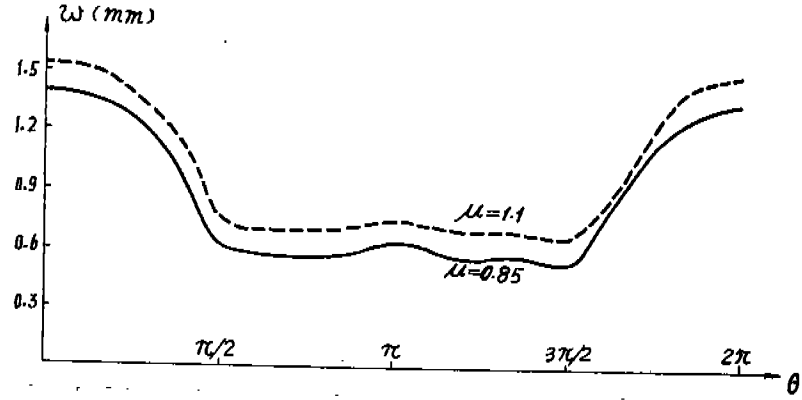

Figure.9. Displacements of valve-plate with variation of gas force (impact at $\theta = 0$, t=0.00125 sec.)

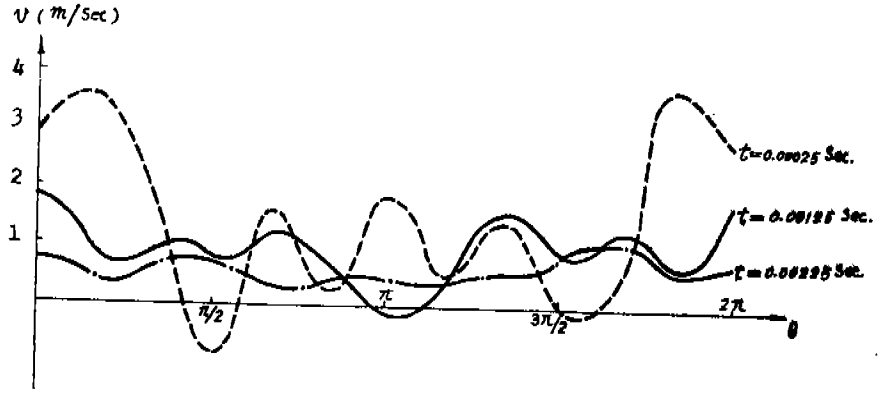

Figure.10. Distribution of valve-plate's circumferented velocities at various instents of time (impact at $\theta = 0$)